Generalized mean-field approach to a resonant Bose-Fermi mixture

D. C. E. Bortolotti,[1,2] A. V. Avdeenkov,[3] and J. L. Bohn[1]
[1]*JILA, NIST and Department of Physics, University of Colorado, Boulder, Colorado 80309-0440, USA*
[2]*Quantitative and Modelling Systems Team, Old Mutual Asset Managers, 2 Lambeth Hill, EC4P 4WR London, United Kingdom*
[3]*Institute of Nuclear Physics, Moscow State University, Vorob'evy Gory, 119992 Moscow, Russia*
(Received 15 September 2008; published 17 December 2008)

We formulate a generalized mean-field theory of a mixture of fermionic and bosonic atoms, in which the fermion-boson interaction can be controlled by a Feshbach resonance. The theory correctly accounts for molecular binding energies of the molecules in the two-body limit, in contrast to the most straightforward mean-field theory. Using this theory, we discuss the equilibrium properties of fermionic molecules created from atom pairs in the gas. We also address the formation of molecules when the magnetic field is ramped across the resonance, and we present a simple Landau-Zener result for this process.

DOI: 10.1103/PhysRevA.78.063612 PACS number(s): 03.75.Hh

I. INTRODUCTION

The use of magnetic Feshbach resonances to manipulate the interactions in ultracold quantum gases has greatly enriched the study of many-body physics. Notable examples include the crossover between BCS (Bardeen-Cooper-Schrieffer [1]) and BEC (Bose-Einstein condensate [2,3]) superfluidity in ultracold Fermi gases [4–6], and the "Bose Nova" collapse in Bose gases [7]. Recent experimental developments [8–13], have enabled the creation of an ultracold mixture of bosons and fermions, where an interspecies Feshbach resonance may introduce a rich source of new phenomena. From the theoretical point of view, studies of Bose-Fermi mixtures to date have been mostly limited to nonresonant physics, focusing mainly on mean-field effects in trapped systems [14–24], phases in optical lattices [25–30], or equilibrium studies of homogeneous gases, focusing mainly on phonon-induced superfluidity or beyond-mean-field effects [31–37]. Pioneering theoretical work on the resonant gas includes Ref. [38], in which a mean-field equilibrium study of the gas is supplemented with a beyond-mean-field analysis of the bosonic depletion; and Ref. [39], where an equilibrium theory is developed using a separable-potentials model.

The aim of this paper is to develop and solve a mean-field theory describing an ultracold atomic Bose-Fermi mixture in the presence of an interspecies Feshbach resonance. This goal appears innocuous enough at first glance, since mean-field theories for resonant Bose-Bose [40,41] and Fermi-Fermi [42–44] gases exist, and have been studied extensively. In both of these theories, the mean-field approximation consists of considering the bosonic Feshbach molecules as being fully condensed, and this greatly simplifies the treatment, since the Hamiltonian reduces to a standard Bogoliubov-like integrable form [45].

The fundamental difference between these examples and the Bose-Fermi mixtures is that in the latter, the Feshbach molecules are fermions, and therefore their center-of-mass momentum must be included explicitly. The most obvious mean-field approach consists in considering the atomic Bose gas to be fully condensed. However, as we will show below, resonant molecules are really composed of two bound atoms, which spend their time together vibrating around their center of mass. It follows that outright omission of the bosonic fluctuations of the atoms disallows the bosonic constituents to oscillate (i.e., fluctuate) at all, and therefore this leads to an improper description of the physics of atom pairs.

This paper is organized as follows. In Sec. II, we introduce the field theory model used to study Feshbach resonances, describing briefly the parametrization used, and outlining the exact solution of this model in the two-body limit. The section ends with a test of this two-body theory by comparing the binding and resonance energies predicted by the model and the virtually exact analogues obtained from two-body close-coupling calculations. Section III introduces the simplest mean-field many-body theory of the gas, obtained by disregarding all bosonic fluctuations. The solution of the theory is outlined, and its limitations highlighted. In spite of these limitations, mean-field theory provides a useful language for dealing with the problem, the utility of which will persist even beyond the limits of applicability of the theory itself.

Finally, in Sec. IV we introduce our generalized mean-field theory, which is, in short, similar to the mean-field theory described in Sec. III, but with the notable improvement of using properly renormalized molecules as building blocks, instead of their bare counterparts. This approach is not trivially described in the Hamiltonian formalism, where substituting dressed molecules for free ones would lead to double counting of diagrams. In this section, we therefore shift to the Green-function–path-integral language, where this double-counting can be avoided quite easily. Finally, we proceed to the numerical solution of this theory, and note that for narrow resonances the results are consistent with their mean-field equivalents. This encourages us to develop a simple theory to study the molecular formation via magnetic field ramps, and, using an approach based on the Landau-Zener formalism [46,47], we derive analytic expressions in Sec. V.

Throughout this paper, we work with zero-temperature gases in the free-space thermodynamic limit. These are limitations that render the results obtained here hard to directly compare with experimental results. One of the main possible future directions of this work should include solving the same problem in a trap, and generalization to higher temperatures.

II. THE MODEL

We are interested primarily in the effects of resonant behavior on the otherwise reasonably understood properties of the system. To this end, we use a model that has become standard in the past few years. This model has been useful in studying the effect of resonant scattering in Bose [41,48,49] and Fermi [50–55] gases. In the case of the Bose-Fermi mixture, this model has been used in Refs. [38,56,57]. We refer to these works for further details about the origin and justification of the Hamiltonian we use here, and for details on the solution in the two-body regime.

The Hamiltonian for the system reads

$$H = H_0 + H_I, \tag{1}$$

where

$$H_0 = \sum_p \epsilon_p^F \hat{a}_p^\dagger \hat{a}_p + \sum_p \epsilon_p^B \hat{b}_p^\dagger \hat{b}_p + \sum_p (\epsilon_p^M + \nu)\hat{c}_p^\dagger \hat{c}_p + \frac{\gamma}{2V}\sum_{p,p',q} \hat{b}_{p-q}^\dagger \hat{b}_{p'+q}^\dagger \hat{b}_p \hat{b}_{p'},$$

$$H_I = \frac{V_{\mathrm{bg}}}{V}\sum_{p,p',q} \hat{a}_{p-q}^\dagger \hat{b}_{p'+q}^\dagger \hat{a}_p \hat{b}_{p'} + \frac{g}{\sqrt{V}}\sum_{q,p} (\hat{c}_q^\dagger \hat{a}_{-p+q/2} \hat{b}_{p+q/2} + \mathrm{H.c.}). \tag{2}$$

Here $\hat{a}_p$, $\hat{b}_p$, are the annihilator operators for, respectively, fermions and bosons, and $\hat{c}_p$ is the annihilator operator for the molecular field [50,54,55]; $\gamma = 4\pi a_b/m_b$ is the interaction term for bosons, where a_b is the boson-boson scattering length; V_{bg}, ν, and g are parameters related to the Bose-Fermi interaction, yet to be determined; the single-particle energies are $\epsilon^\alpha = p^2/2m_\alpha$, where m_α indicates the mass of bosons, fermions, or pairs; and V is the volume of a quantization box with periodic boundary conditions.

The first step is to find the values for V_{bg}, ν, g, in terms of measurable parameters. We will, for this purpose, calculate the two-body T-matrix resulting from the Hamiltonian in Eq. (2). Integrating the molecular field out of the real-time path integral leads to the following Bose-Fermi interaction Hamiltonian:

$$H_I^{\text{two body}} = \frac{1}{V}\left(V_{\mathrm{bg}} + \frac{g^2}{E-\nu}\right)\sum_p \hat{a}_p^\dagger \hat{b}_{-p}^\dagger \hat{a}_p \hat{b}_{-p}. \tag{3}$$

This expression is represented in center-of-mass coordinates, and E is the collision energy of the system. From the above equation, we read trivially the zero-energy scattering amplitude in the saddle-point approximation,

$$T = \left(V_{\mathrm{bg}} - \frac{g^2}{\nu}\right), \tag{4}$$

which corresponds to the Born approximation (this is akin to identifying the scattering amplitude $f = a_{\mathrm{sc}}$ in the Gross-Pitaevskii equation, where the interaction term would be $\frac{2\pi}{m_{\mathrm{bf}}}a_b$). We emphasize that this approximation is only valid in the zero-energy limit, and it does not, therefore, describe the correct binding energy as a function of detuning. However, with this approach we obtain an adequate description of the behavior of scattering length as a function of detuning, which allows us to relate the parameters of our theory to experimental observables via the conventional parametrization [48,50]

$$T(B) = \frac{2\pi}{m_{\mathrm{bf}}} a_{\mathrm{bg}}\left(1 - \frac{\Delta_B}{(B-B_0)}\right), \tag{5}$$

where a_{bg} is the value of the scattering length far from resonance, Δ_B is the width, in magnetic field, of the resonance, m_{bf} is the reduced mass, and B_0 is the field at which the resonance is centered.

The identification of parameters between Eqs. (4) and (5) proceeds as follows: far from resonance, $|B-B_0| \gg \Delta_B$, the interaction is defined by a background scattering length, via $V_{\mathrm{bg}} = \frac{2\pi a_{\mathrm{bg}}}{m_{\mathrm{bf}}}$. To relate the magnetic-field-dependent quantity $B-B_0$ to its energy-dependent analog ν requires defining a parameter $\delta_B = \partial\nu/\partial B$, which may be thought of as a kind of magnetic moment for the molecules. It is worth noting that ν does not represent the position of the resonance nor the binding energy of the molecules, and that, in general, δ_B is a field-dependent quantity, since the thresholds move quadratically with field because of nonlinear corrections to the Zeeman effect. For current purposes, we identify δ_B by its behavior far from resonance, where it is approximately constant. Careful calculations of scattering properties using the model in Eq. (2), however, lead to the correct Breit-Wigner behavior of the two-body T-matrix [58].

Finally, we get the following identifications:

$$V_{\mathrm{bg}} = \frac{2\pi a_{\mathrm{bg}}}{m_{\mathrm{bf}}},$$

$$g = \sqrt{V_{\mathrm{bg}}\delta_B\Delta_B},$$

$$\nu = \delta_B(B-B_0). \tag{6}$$

Synthesizing the approach described in [56], and diagrammatically represented in Fig. 1, we can obtain the exact two-body T-matrix of the system by solving the Dyson equation

$$T = gD^0g + gD^0g\Pi gD^0g + gD^0g\Pi gD^0g\Pi gD^0g + \cdots = gDg, \tag{7}$$

where T is the T-matrix for the collision, and which has the formal solution

$$T = gDg = \frac{g^2}{(D^0)^{-1} - g^2\Pi}. \tag{8}$$

These quantities take the explicit form

$$D^0(E) = \left(\frac{V_{\mathrm{bg}}}{g^2} + \frac{1}{E-\nu}\right), \tag{9}$$

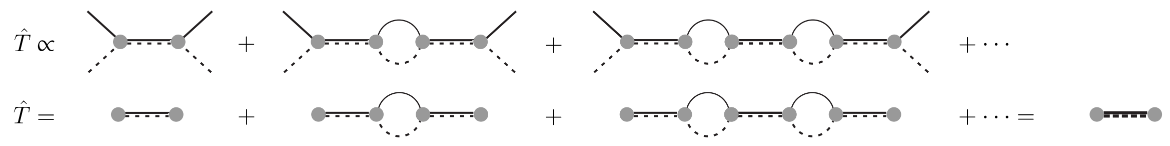

$$\hat{T} = g\,\hat{D}^0\,g + g\,\hat{D}^0\,g\,\hat{\Pi}\,g\,\hat{D}^0\,g + g\,\hat{D}^0\,g\,\hat{\Pi}\,g\,\hat{D}^0\,g\,\hat{\Pi}\,g\,\hat{D}^0\,g + \cdots = g\,\hat{D}\,g$$

FIG. 1. Feynman diagrams representing the resonant collision of a fermion and a boson. Solid lines represent fermions, dashed lines bosons, and double solid-dashed lines represent the effective composite fermions.

$$\Pi(E) = -i\int \frac{d\omega}{2\pi}\frac{d\mathbf{p}}{(2\pi)^3}\frac{1}{\left(\hbar\omega - \frac{p^2}{2m_b} + i0^+\right)} \times \frac{1}{\left(E - \hbar\omega - \frac{p^2}{2m_f} + i0^+\right)} \approx i\frac{m_{\mathrm{bf}}^{3/2}}{\sqrt{2}\pi}\sqrt{E} + \frac{m_{\mathrm{bf}}\Lambda}{\pi^2}, \tag{10}$$

where m_{bf} is the boson-fermion reduced mass and Λ is an ultraviolet momentum cutoff needed to hide the unphysical nature of the contact interactions. Note that D^0 represents an effective molecular field, accounting for the fermion-boson background interaction, and, as described in detail in [56], it is obtained by integrating the original molecular field, and performing a Hubbard-Stratonovich transformation [59] to eliminate the direct boson-fermion interaction in favor of the effective molecular field D^0.

Regularization of the theory [42,56] is obtained by the substitutions

$$\overline{V_{\mathrm{bg}}} = V_{\mathrm{bg}}\left(\frac{1}{1 - \frac{m_{\mathrm{bf}}\Lambda V_{\mathrm{bg}}}{\pi^2}}\right)$$

$$\bar{g} = g\left(\frac{1}{1 - \frac{m_{\mathrm{bf}}\Lambda V_{\mathrm{bg}}}{\pi^2}}\right)$$

$$\bar{\nu} = \nu + \bar{g}g\frac{m_{\mathrm{bf}}\Lambda V_{\mathrm{bg}}}{\pi^2}. \tag{11}$$

Finally the two-body T-matrix takes the form

$$T(E) = \left[\frac{1}{V_{\mathrm{bg}} + \frac{g^2}{E-\nu}} + i\frac{m_{\mathrm{bf}}^{3/2}}{\sqrt{2}\pi}\sqrt{E}\right]^{-1}. \tag{12}$$

Poles of the T-matrix: Testing the model

Bound states and resonances of the two-body system are identified in the structure of poles of the T-matrix [Eq. (12)]. This is illustrated in Fig. 2, where real and imaginary parts of the poles' energies are plotted as a function of magnetic field. The resonance portrayed in the figure is the 544.7 G resonance present in the $|9/2,-9/2\rangle|1,1\rangle$ state of ^{40}K-^{87}Rb. For $B<544.7$ G (corresponding to detunings $\nu<0$), the two-body system possesses a true bound state, whose binding energy is denoted by the solid line. In this case, the pole occurs for real energies. This bound state vanishes as the detuning goes to zero, where the resonance occurs.

For positive detunings, $\nu>0$, on the other hand, the poles are complex, and the inverse of the imaginary part is proportional to the lifetime of the metastable resonant state.

In this regime, there is no longer a true bound state, but there may be a scattering resonance, indicated in Fig. 2 by a thick dashed line. This resonance appears for magnetic fields $B>544.7$ G for this particular resonance, well before the disappearance of the bound state. This value is highly dependent upon the value of the background potential. We will see in Sec. IV that for $V_{\mathrm{bg}}=0$, the resonance actually appears at positive detunings. In the case of ^{40}K-^{87}Rb, $V_{\mathrm{bg}}<0$, implying that there is a weak potential resonance in the open channel that interferes with the closed-channel resonance, and causes it to cross the axis at negative detunings. For $V_{\mathrm{bg}}>0$ (Ref. [60]), the positive background scattering length is set by a bound state in the open channel, which does not affect the resonance states, but which interferes with the bound state at negative detunings.

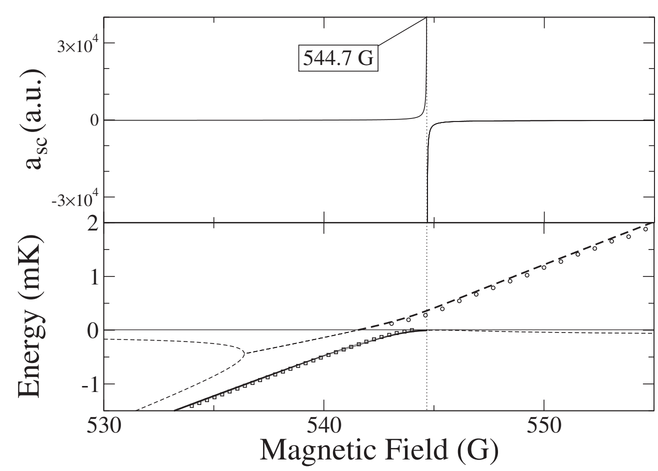

FIG. 2. The top panel shows the scattering length versus magnetic field for the 544.7 G resonance, present in the $|9/2,-9/2\rangle|1,1\rangle$ states of the ^{40}K-^{87}Rb collision. The bottom panel shows the poles of the model two-body T-matrix [Eq. (12)] parametrized for the same resonance, as a function of magnetic field. Thick solid and dashed lines denote the real parts of relevant poles, representing bound and resonance states, respectively. The thin dashed lines are the real parts of unphysical poles. The empty circles and squares represent the position of the resonance and the bound state, obtained via a virtually exact close-coupling calculation, and are presented to show the level of accuracy of the model.

The thin dashed lines in Fig. 2 are a physically meaningless solutions to the Schrödinger equation, in which the amplitude in the resonant state would grow exponentially in time, rather than decay. These poles do not, therefore, identify any particular features in the energy-dependent cross section of the atoms, and will not modify the physics of the system. Finally, Fig. 2 contains data obtained from virtually exact close-coupling calculations that show the extent of validity of the model. For the purposes at hand, this agreement is sufficient.

It should be noted that the agreement is not as good for positive background scattering length systems, since the open-channel bound state determining this scattering length is not adequately described by the model, which treats the background physics as an essentially zero-range interaction. This implies that the relation between the background scattering length and open channel bound-state energy is exactly $E_b = 1/2\mu a_{\rm bg}^2$, while in the physical system this relation depends on the details of the interaction potential. This problem has been addressed in the literature [61], but no treatable field theory has yet been proposed.

III. MEAN-FIELD THEORY

In this section, we introduce the many-body physics of the system by first analyzing it in a mean-field approach. Because of the statistical properties of the system, we will see right away that mean-field theory does not recover the correct two-body physics in the low-density limits. In spite of this substantial weakness, however, the approach has several qualitative features that persist even in the improved theory that we introduce below. Furthermore, since the model is exactly solvable, it will allow us to develop a language that will help us to understand the problem in simpler terms, and to identify some small physical effects, which, when ignored, can greatly simplify the beyond mean-field approach presented in the next section.

A. The formalism

Starting with the Hamiltonian described by Eq. (1), we obtain the mean-field Hamiltonian by substituting the boson annihilator $\hat{b}$ by its expectation value $\phi = \langle \hat{b} \rangle$, a complex number. The number operator $\hat{b}_p^\dagger \hat{b}_p$, therefore, becomes $|\phi|^2 = N_b$, where N_b is the number of condensed bosons. The grand-canonical Hamiltonian, therefore, becomes

$$H = E_b + \sum_p (\epsilon_p^F - \mu_f + V_{\rm bg} n_b) \hat{a}_p^\dagger \hat{a}_p + \sum_p (\epsilon_p^M + \nu - \mu_m) \hat{c}_p^\dagger \hat{c}_p + g\sqrt{n_b} \sum_p (\hat{c}_p^\dagger \hat{a}_p + \text{H.c.}), \tag{13}$$

where n_b is the density of condensed bosons, $E_b/V = \gamma n_b^2 - \mu_b n_b$ is the energy per unit volume of the (free) condensed bosons, a constant contribution to the total energy of the system, and $\mu_{(b,f,m)}$ are the chemical potentials. These are Lagrange multipliers that serve to keep the densities constant as we minimize the energy to find the ground state. In the following we will drop the volume term, absorbing it in the definition of the creation and annihilation operators, such that the expected value of the number operator represents a density, instead of a number.

Before proceeding with the analysis of this Hamiltonian, we introduce the set of self-consistent equations we wish to solve. To this end, we define the quantities $n_{b(f)}^0$, representing the total density of bosons (fermions) in the system, at detuning $\nu \to \infty$. At finite detunings, some of these atoms will combine into molecules, and the densities will be denoted as $n_{(b,f,m)}$ for bosons, fermions, and molecules, respectively.

The system, therefore, is described by six quantities, namely three densities and three chemical potentials, which require six equations to determine. These equations, which can be derived by number-conservation constraints and energy minimization arguments, are

$$n_f + n_m - n_f^0 = 0, \tag{14a}$$

$$n_b + n_m - n_b^0 = 0, \tag{14b}$$

$$n_f = \frac{d\Omega}{d\mu_f}, \tag{14c}$$

$$n_m = \frac{d\Omega}{d\mu_m}, \tag{14d}$$

$$\frac{d\Omega}{d\phi} = 0, \tag{14e}$$

$$\mu_b + \mu_f = \mu_m, \tag{14f}$$

where $\Omega = \langle H \rangle / V$ is the Gibbs free energy. Equations (14a) and (14b) follow from the simple counting argument that for every molecule created, there is one less free boson and one less free fermion in the gas. Equations (14c) and (14d) are simply the Lagrange multiplier constraint equations, Eq. (14e) follows from the mean-field approximation, whereby the bosonic field is simply a complex number, and minimization of the energy can therefore be done directly. Finally, Eq. (14f) is the law of mass action, which follows from the fact that to make a molecule, it takes one free atom of each kind.

The next step is to write down Ω for the system by taking the expectation value of the Hamiltonian in Eq. (13), obtaining

$$\Omega = E_b/V + \sum_p (\epsilon_p^F - \mu_f + V_{\rm bg} n_b) \eta_f(p) + \sum_p (\epsilon_p^M + \nu - \mu_m) \eta_m(p) + 2g\sqrt{n_b} \sum_p \eta_{mf}(p), \tag{15}$$

where $\eta_f(p) = \langle \hat{a}_p^\dagger \hat{a}_p \rangle$ and $\eta_m(p) = \langle \hat{c}_p^\dagger \hat{c}_p \rangle$ are the fermionic and molecular momentum distributions, $\eta_{\rm mf}(p) = \langle \hat{c}_p^\dagger \hat{a}_p \rangle$ is an off-diagonal correlation term arising from the interactions in the system, and the densities are given by $n_{f,m,{\rm mf}} = \int \frac{dp}{2\pi^2} \eta_{f,m,{\rm mf}}(p)$. Equations (14a)–(14f) then read

$$n_f + n_m - n_f^0 = 0, \tag{16a}$$

$$n_b + n_m - n_b^0 = 0, \tag{16b}$$

$$n_{f,m,\mathrm{mf}} = \int \frac{dp}{2\pi^2}\,\eta_{f,m,\mathrm{mf}}(p), \tag{16c}$$

$$g n_{\mathrm{mf}} - \mu_b\sqrt{n_b} + \gamma n_b^{3/2} = 0, \tag{16d}$$

$$\mu_b + \mu_f = \mu_m. \tag{16e}$$

The remaining task is now to find expressions to calculate the expected values $\eta_{f,m,\mathrm{mf}}(p)$. To this end, we follow a Bogoliubov-like approach, similar to that described in [38]. The mean-field Hamiltonian is bilinear in all creation and annihilation operators, which means that it can be diagonalized via a change of basis, whereby introducing the operators

$$\hat{\alpha}_p = A_\alpha \hat{a}_p + C_\alpha \hat{c}_p,$$

$$\hat{\beta}_p = A_\beta \hat{a}_p + C_\beta \hat{c}_p, \tag{17}$$

for some appropriately chosen coefficients $A_{\alpha,\beta}$ and $B_{\alpha,\beta}$, the Hamiltonian will read

$$H' = E_0 + \sum_p \lambda_\alpha(p)\hat{\alpha}_p^\dagger\hat{\alpha}_p + \sum_p \lambda_\beta(p)\hat{\beta}_p^\dagger\hat{\beta}_p. \tag{18}$$

At this point, we note that the Hamiltonian is just a separable sum of free-particle Hamiltonians, where the free particles are fermions with dispersion relations $\lambda_{\alpha,\beta}(p)$. We can readily write down the distribution

$$\eta_{\alpha,\beta}(p) = \Theta(-\lambda_{\beta,\alpha}(p)), \tag{19}$$

where Θ is the step function, and we calculate the densities $n_{\alpha,\beta}$. The step function could be replaced by the free Fermi distribution for nonzero temperatures, but the mean-field assumption that all bosons are condensed would no longer hold. If these were ordinary free fermions with dispersion $p^2/2m-\mu$, Eq. (19) would reduce to the standard zero-temperature Fermi distribution. We will see below that $\lambda_{\alpha,\beta}(p)$ are dispersion relations of quasiparticles that are a mixture of atoms and molecules.

Below we show how these ideas, together with Eqs. (14a)–(14f), give us the tools we require to calculate the observable atomic and molecular densities as a function of the chemical potentials.

To illustrate more explicitly the diagonalization procedure, we define the vectors

$$A = \begin{pmatrix} \hat{a}_p \\ \hat{c}_p \end{pmatrix}, \quad A^\dagger = (\hat{a}_p^\dagger \hat{c}_p^\dagger), \tag{20}$$

and

$$B = \begin{pmatrix} \hat{\alpha}_p \\ \hat{\beta}_p \end{pmatrix}, \quad B^\dagger = (\hat{\alpha}_p^\dagger \hat{\beta}_p^\dagger), \tag{21}$$

whereby the Hamiltonian can be written as $A^\dagger \hat{H} A$ and $B^\dagger \hat{H}' B$, where

$$\hat{H} = \begin{pmatrix} (\epsilon_p^F - \mu_f + V_{\mathrm{bg}} n_b) & g\sqrt{n_b} \\ g\sqrt{n_b} & (\epsilon_p^M + \nu - \mu_m) \end{pmatrix} \tag{22}$$

and

$$\hat{H}' = \begin{pmatrix} \lambda_\alpha(p) & 0 \\ 0 & \lambda_\beta(p) \end{pmatrix}. \tag{23}$$

Diagonalizing $\hat{H}$, we get the two eigenvalues

$$\lambda_{\alpha,\beta}(p) = \frac{h_f(p)+h_m(p)}{2} \pm \frac{1}{2}\sqrt{4g^2 n_b + [h_m(p)-h_f(p)]^2}, \tag{24}$$

where we have defined $h_f(p)=(\epsilon_p^F-\mu_f+V_{\mathrm{bg}}n_b)$ and $h_m(p)=(\epsilon_p^M+\nu-\mu_m)$, and the unitary eigenvector matrix

$$U = \begin{pmatrix} A_\alpha & B_\alpha \\ A_\beta & B_\beta \end{pmatrix}. \tag{25}$$

The transformation in Eq. (17) can then be written as $A=U^\dagger B$, and its inverse $B=UA$.

Our goal now is to write the densities $\eta_{m,f,\mathrm{mf}}(p)$ in terms of the known densities $\eta_{\alpha,\beta}(p)$. In component notation (where $A_i=\hat{a}_p$, etc.), we can write

$$\langle A_i^\dagger A_l\rangle = \langle B_j^\dagger U_{ji}(U^\dagger)_{lj}B_k\rangle = U_{lj}U_{ij}^*\langle B_j^\dagger B_j\rangle, \tag{26}$$

where we have used the fact that since the Hamiltonian is diagonal in the B basis, then $\langle B_j^\dagger B_k\rangle=\langle B_j^\dagger B_j\rangle\delta_{jk}$.

Using this formalism, we obtain the relations

$$\eta_f(p) = |A_\alpha|^2\eta_\alpha(p) + |B_\alpha|^2\eta_\beta(p),$$

$$\eta_f(p) = |A_\beta|^2\eta_\alpha(p) + |B_\beta|^2\eta_\beta(p),$$

$$\eta_{fm}(p) = A_\alpha^* A_\beta \eta_\alpha(p) + B_\alpha^* B_\beta \eta_{\varrho ta}(p). \tag{27}$$

Using these expressions in conjunction with Eqs. (16a)–(16e) will then allow us to compute the equilibrium properties of the system.

This simplified, mean-field version of the solution can only approximately reproduce the energies of atomic and molecular states, as is shown in Fig. 3. In this example, we have assumed a uniform mixture of ^{40}K and ^{87}Rb atoms with densities 8.2×10^{14} cm^{-3} and 4.9×10^{15} cm^{-1}, respectively. These densities correspond to the central density of each species assuming it is confined to a 100 Hz spherical trap. Far from the resonance, these energies asymptote to zero (representing the atomic state) and to the detuning (representing the bare molecular state that went into the theory). Near zero detuning, these levels cross owing to the coupling term $g\sqrt{n_b}$ in Eq. (22). The size of this crossing is therefore larger the larger the bosonic density is. In the crossing region, the eigenstates do not clearly represent either atoms or molecules, but linear combinations of the two.

B. Mean field: Noninteracting case

To better understand the structure of the mean-field theory, in this section we detail its results for a *noninteract-*

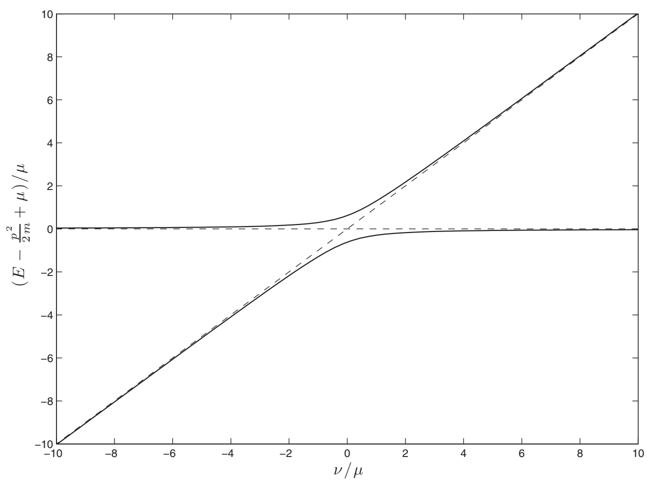

FIG. 3. The thick solid lines represent the "renormalized" mean-field energy levels $\lambda_{\alpha,\beta}(k_f)$, while the thin dashed lines represent their bare counterparts.

ing gas by setting $g=V_{\mathrm{bg}}=\gamma=0$. We contrast two different physical regimes, based on the ratio of bosons to that of fermions, $r_{\mathrm{bf}}\equiv n_b/n_f$.

In the case of high fermion density, we set $r_{\mathrm{bf}}=0.6$, and plot chemical potentials and populations of the various states in Fig. 4. Consider what happens in an infinitely slow ramp from positive detuning (no molecules) to negative detuning

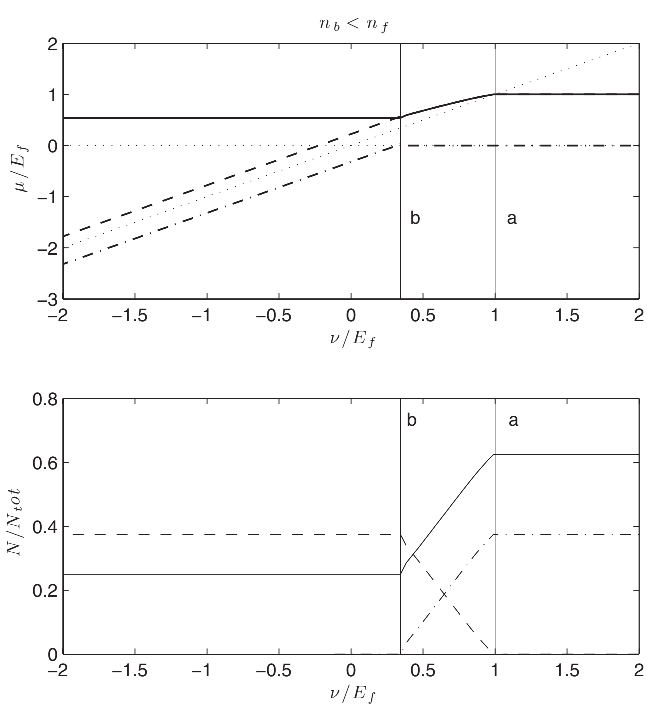

FIG. 4. Equilibrium chemical potentials (top panel) and populations (bottom panel) as a function of detuning for a noninteracting gas with $r_{\mathrm{bf}}=0.6$. The solid lines represent fermions, dashed lines molecules, and dashed-dotted lines bosons. The dotted lines in the top panel represent the bare molecular and fermionic internal energies, respectively, ν and 0. The vertical lines labeled (a) and (b) are discussed in the text, and represent the detuning at which molecular formation begins and ends, respectively.

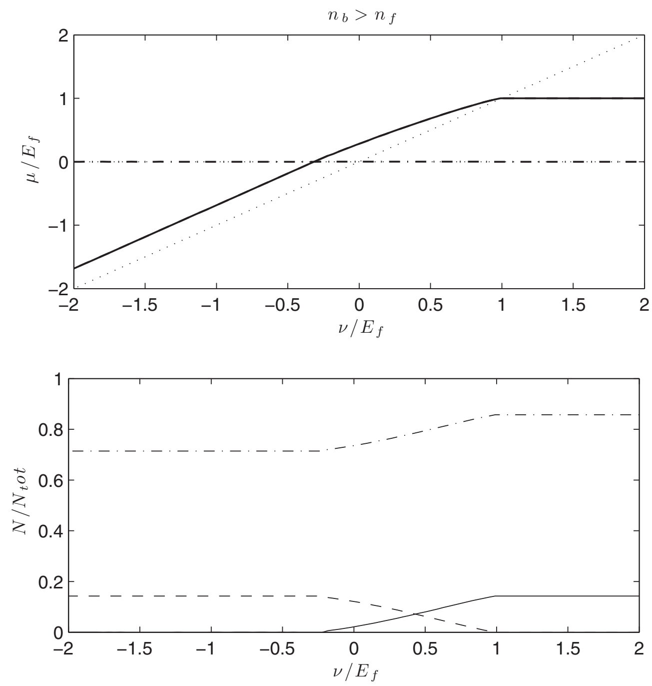

FIG. 5. Equilibrium chemical potentials (top panel) and populations (bottom panel) as a function of detuning for a noninteracting gas with $r_{\mathrm{bf}}=6$. The solid lines represent fermions, dashed lines molecules, and dashed-dotted lines bosons. The dotted lines in the top panel represent the bare molecular and fermionic internal energies, respectively, ν and 0.

(introducing bound molecular states). For large positive detuning, the fermionic and molecular chemical potentials are the same, since the chemical potential of the condensed bosons vanishes. For large enough detuning, the molecular chemical potential remains below the detuning, so it is energetically unfavorable to make molecules. When the detuning dips below the chemical potential (detuning *a* in the figure), fermions begin to pair with bosons to make molecules (see populations in lower panel). This process continues until all the bosons are consumed (detuning *b*), at which point the populations stabilize. For detunings less than this, there remain both fermions and fermionic molecules in the gas, and there are two Fermi surfaces present. Because the internal energy of the molecules continues to diminish at lower detuning, so does the molecular chemical potential. The two Fermi surfaces, therefore, split from one another, although the relative population of the two fermions is fixed.

By contrast, the case in which the bosons outnumber the fermions is shown in Fig. 5, where we have set the density ratio to $r_{\mathrm{bf}}=6$. As in the previous case, no molecules are generated until the detuning drops lower than the chemical potential of the atomic Fermi gas. Since there are enough bosons to turn all the fermions into molecules, there are no fermionic atoms at sufficiently negative detuning, and the gas possesses only a single Fermi surface. The chemical potential of the remaining bosons is still zero, since these bosons are condensed. Formally, then, the chemical potential for atomic fermions is negative, meaning that their formation at negative detuning is energetically forbidden.

TABLE I. Parametrization of the three main Feshbach resonances used in this thesis. All three resonances are in the $|9/2,-9/2\rangle|1,1\rangle$ states of the ^{40}K-^{87}Rb collision.

B_0 (G)	Δ_B (G)	δ_B (K/G)	a_{bg} (a.u.)
492.49	0.134	3.624×10^{-5}	−176.5
544.7	3.13	1.576×10^{-4}	−176.5
659.2	1.0	2.017×10^{-4}	−176.5

C. Mean field: Interacting case

In most experimental circumstances, the density of bosons is larger than that of fermions, since condensed bosons cluster to the center of the trap, whereas fermions are kept away by Pauli blocking. We therefore focus on this case hereafter, setting the Bose and Fermi densities to $n_b=4.9\times10^{15}$ cm^{-3} and $n_f=8.2\times10^{14}$ cm^{-3}. The coupling term $g\sqrt{n_b}$ in Eq. (22) is the perturbative expansion parameter for the problem, and since it has units of energy, it must be compared with the characteristic nonperturbed energy of the gas, which in this case is E_f. Also since in the perturbative expansions it always appears squared [see Eq. (7)], we can define the unitless small parameter for the system as $\epsilon_{\mathrm{SM}}=g^2n_b/E_f^2=g^2n_f/E_f^2r_{\mathrm{bf}}$. For the 492 G resonance in Table I, we have $\epsilon_{\mathrm{SM}}=6.35\times10^{-2}r_{\mathrm{bf}}$, and since $r_{\mathrm{bf}}=6$, the small parameter is of order 0.1, appropriate for perturbative treatment.

Figure 6 shows the equilibrium chemical potentials for the system obtained via a self-consistent solution of Eqs. (28) and (16a)–(16e). This figure is qualitatively similar to the corresponding noninteracting result in Fig. 5, but contains important differences. First, the nonzero boson-boson interaction generates a nonzero bosonic chemical potential μ_b that breaks the degeneracy between the molecular and fermionic chemical potentials. In physical terms, this means that there is an energy cost in maintaining bosons unpaired, and therefore we need to take this into account in the kinematic analysis. Namely, to make molecules energetically favorable no longer requires a detuning ν such that $\nu=\mu_f$, but now requires $\nu=\mu_f+\mu_b$. The net result is to shift the chemical potential up and to the left by an amount μ_b, and to shift the molecular population curve to the left by this amount.

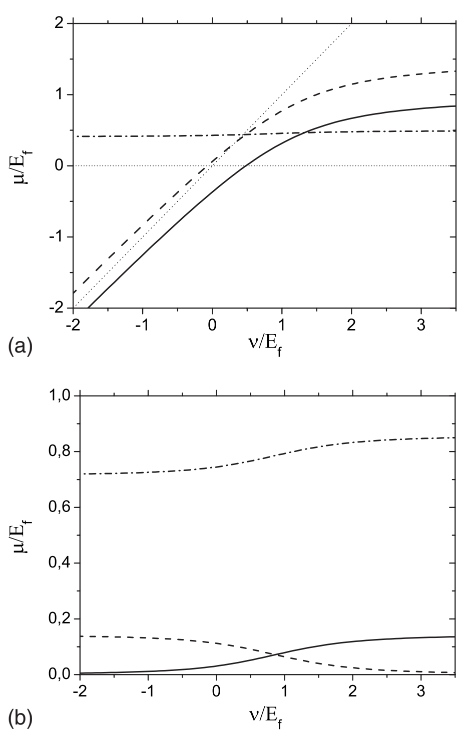

FIG. 6. Mean-field equilibrium chemical potentials (top panel) and populations (bottom panel) as a function of detuning. The solid lines represent fermions, dashed lines molecules, and dashed-dotted lines bosons.

A second difference is that molecule creation takes place more gradually as a function of detuning in the interacting case. This is simply the result of the avoided crossing smearing out the molecular energy.

Finally, we exploit the simplicity of the mean-field approach to test some approximations that will simplify the beyond-mean-field approach in the next section. These approximations have been tested numerically, and they give corrections of the order of 0.1% or less in calculated molecular populations for all regimes of interest here. The approximations are (i) incorporate the boson-boson interaction γN_b^3 by shifting the detuning and chemical potential as discussed above; (ii) disregard the background scattering between bosons and fermions, i.e., set $V_{\mathrm{bg}}=0$, since this interaction is dominated by its resonance part; and (iii) disregard the correlation function $\langle\eta_b f(p)\rangle$ (analogous to the boson polarization operator in the Green-function formalism), since its contribution to μ_b is much smaller than that of γn_b^3. It is difficult to directly verify the validity of these approximations in the beyond-mean-field approach. Nevertheless, we expect that these approximations remain valid, since the generalized mean-field theory is, after all, a mean-field theory at heart.

IV. GENERALIZED MEAN-FIELD THEORY

In Sec. III, we reached the conclusion that the mean-field approach to the resonant Bose-Fermi system does not properly account for the correct two-body physics of the system. In this section, we wish to improve on this by introducing a generalization to mean-field theory, via an appropriate renormalization of the molecular propagator, which is able to reproduce the correct two-body physics in the low-density limit. To accomplish this, we will have to abandon the Hamiltonian treatment of the previous section, in favor of a perturbative approach based on the Green's-function formalism, much as was done for two bodies in Sec. II. Throughout this section, we use the approximations made above, namely $\gamma n_b^3=V_{\mathrm{bg}}=\langle\eta_b f(p)\rangle=0$.

We begin by recasting the rn field result from Sec. III in the language of Green functions. The self-consistent Dyson equations that describe this system are

$$G_F^{\mathrm{MF}}(E,P)=G_F^0(E,P)+G_F^0(E,P)g^2n_bD^0(E,P)G_F^{\mathrm{MF}}(E,P),$$

$$D^{\mathrm{MF}}(E,P)=D^0(E,P)+D^0(E,P)g^2n_bG_F^0(E,P)D^{\mathrm{MF}}(E,P), \tag{28}$$

where the free propagators are simply

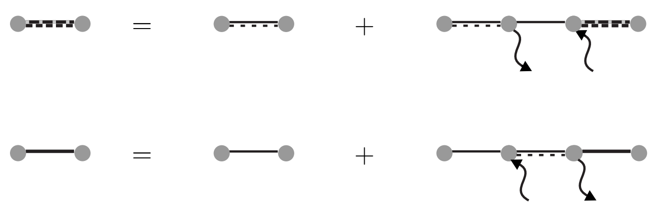

FIG. 7. Feynman diagrams included in the mean-field theory. Thin (thick) solid lines represent free (renormalized) fermions, thin double-dashed–solid lines represent free molecules, and thick double-dashed lines represent renormalized molecules. The little wavy lines represent condensed bosons, whereby the arrow indicates whether they are taken from or released into the condensate.

$$D^0 = \frac{1}{\omega - \xi^M(p) + i\eta\,\mathrm{sgn}[\xi(p)]},$$

$$G_F^0 = \frac{1}{\omega - \xi^F(p) + i\eta\,\mathrm{sgn}[\xi(p)]}, \tag{29}$$

and $\xi^{M,F}(p)=(\epsilon_p^{M,F}-\mu_{m,f})$ These propagators are described diagrammatically in Fig. 7. They represent the fact that a free fermion may encounter a *condensed* boson and associate with it, temporarily creating a molecule; or that a free molecule may temporarily split into a fermion and a condensed boson. Self-consistency ensures that these processes may be repeated coherently an infinite number of times. We neglect the bosonic renormalization equation $\phi^{\mathrm{MF}}=n_b^0+g^2 n_b G_F^0(E,P)D^0(E,P)$, whereby a condensed boson may pick up a fermion to create a molecule; this is equivalent to the condition $\langle \eta_b f(p)\rangle=0$.

Solutions to these equations take the form

$$G_F^{\mathrm{MF}}(E,P) = \frac{1}{G_F^0(E,P)^{-1} - g^2 n_b D^0(E,P)},$$

$$D^{\mathrm{MF}}(E,P) = \frac{1}{D^0(E,P)^{-1} - g^2 n_b G_F^0(E,P)}. \tag{30}$$

Using the definitions of $G_F^0(E,P)$ and $D^0(E,P)$ from Eq. (29), we can find the poles corresponding to many-body bound states. In this case, it can be shown that the poles are exactly the mean-field eigenvalues $\lambda_{\alpha,\beta}(p)$ from Sec. II. Moreover, Eqs. (30) are symmetric with respect to interchange of G_F and D, which implies that both renormalized Green functions have the same poles, and the same residues. We can therefore study the properties of the fermions by only looking at the molecules. This is not completely surprising, since, given that the condensed bosons are relatively inert, every molecule corresponds exactly to a missing fermion, and vice versa.

The most important deficiency of this mean-field approach is that it only allows molecules to decay into a free fermion and a condensed boson, disregarding the possibility that the bosonic by-product may be noncondensed. We must allow noncondensed bosons somehow, and yet these bosons make a perturbation to the result, as seen by the following argument. The fundamental mean-field assumption is that the gas is at zero temperature, and therefore the noncondensed population should be negligible at equilibrium. Furthermore, if a molecule is composed of a zero-momentum boson and a fermion from the Fermi sea, dissociating into a noncondensed boson implies that the outgoing fermion would have momentum lower than the Fermi momentum, an event that Pauli blocking makes quite unlikely. Therefore, if a molecule does indeed decay yielding a noncondensed boson, it should immediately recapture the boson in a virtual process such as that described in Fig. 1. It is only convenient that these events are exactly the kind of events that will correctly renormalize the binding energy of the molecules, leading to a theory that will reproduce the exact two-body resonant physics.

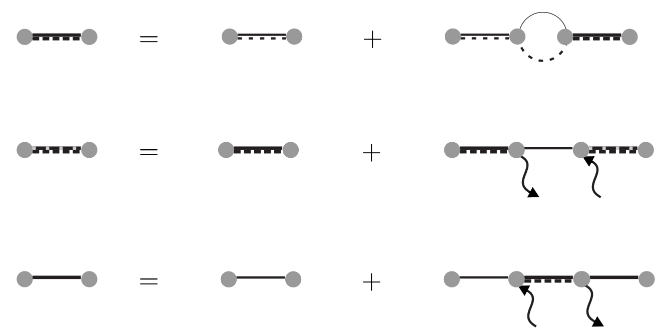

FIG. 8. Feynman diagrams included in the generalized mean-field theory. Like in the mean-field case (Fig. 7), thin (thick) solid lines represent free (renormalized) fermions, thin double-dashed–solid lines represent free molecules, and thick double-dashed lines represent renormalized molecules. The little wavy lines represent condensed bosons, whereby the arrow indicates whether they are taken from or released into the condensate. The novelty here is the inclusion of the two-body dressed molecules from Fig. 1.

The Dyson equations describing this generalized mean-field theory are

$$G_F^{\mathrm{GMF}}(E,P) = G_F^0(E,P) + G_F^0(E,P) g^2 n_b D(E,P) G_F^{\mathrm{GMF}}(E,P),$$

$$D^{\mathrm{GMF}}(E,P) = D(E,P) + D(E,P) g^2 n_b G_F^0(E,P) D^{\mathrm{GMF}}(E,P). \tag{31}$$

Here we have replaced the free propagator D^0 by the renormalized molecular propagator D from Eq. (8). A diagrammatic representation of this theory appears in Fig. 8. By analogy with the mean-field version, the solutions to these equations are

$$G_F^{\mathrm{GMF}}(E,P) = \frac{1}{G_F^0(E,P)^{-1} - g^2 n_b D(E,P)},$$

$$D^{\mathrm{GMF}}(E,P) = \frac{1}{D(E,P)^{-1} - g^2 n_b G_F^0(E,P)}. \tag{32}$$

These equations preserve the symmetrical nature of the mean-field theory described above, and also the avoided crossing of atomic and molecular levels. This is demonstrated in Fig. 9, where we reproduce the $P=k_f$ pole of D from Fig. 2 as dashed lines. We also present in this figure the corresponding poles for the generalized mean-field theory as

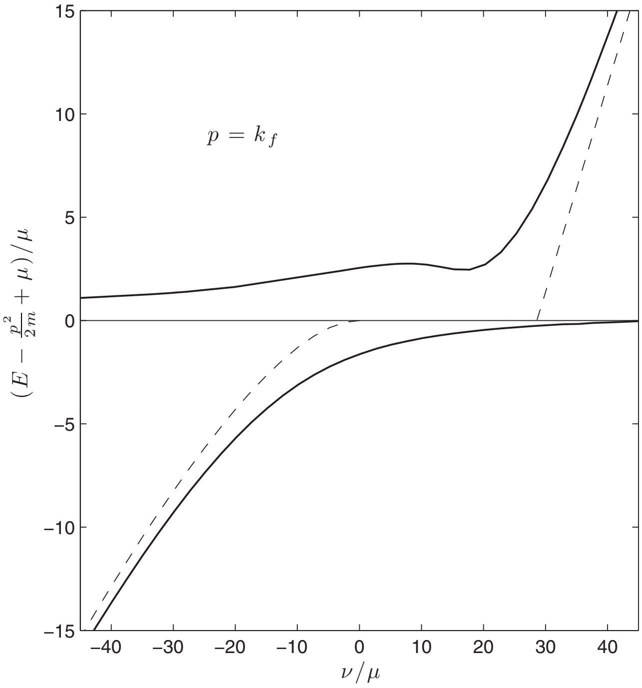

FIG. 9. The thick lines represent the poles of $D^{\mathrm{GMF}}(k_f)$, and correspond to molecular and fermionic energies. The dashed lines represent the molecular two-body poles, corresponding to the molecular binding and resonant energies obtained disregarding the background interaction [57]. As in the mean-field theory case, the effect of the interaction with the condensate is to create an avoided crossing between the atomic and molecular states. The "bulge" in the upper solid curve is a consequence of Pauli blocking, which has the consequence of favoring molecular stability. See [57] for more details.

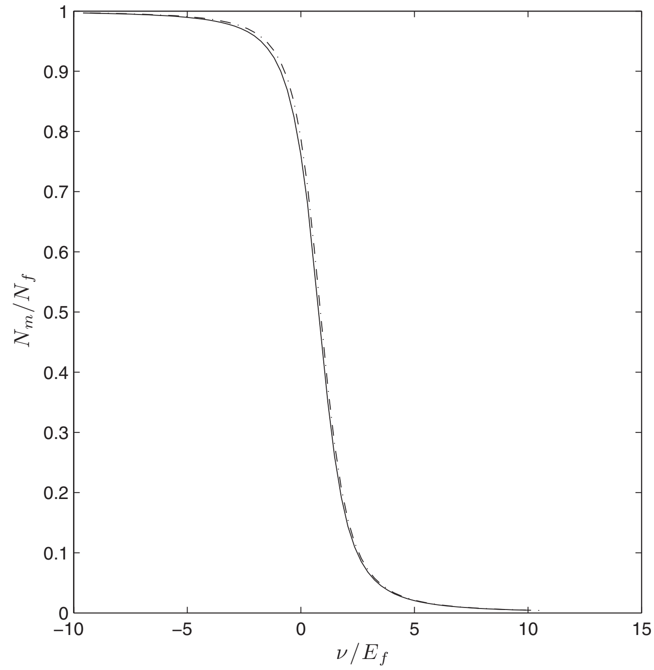

FIG. 10. Equilibrium molecular population as a function of detuning for the narrow 492.49 G resonance. The solid line represents results obtained via the generalized mean-field theory presented in the text, while the dashed-dotted line represents the mean-field results.

solid lines. As in Fig. 3, we note the splitting in two energy levels, avoiding each other around $\nu=0$. The fundamental difference in this case is that the molecular curve does not asymptote to the bare detuning, but rather to the correct molecular binding and resonance energies.

Studying the equilibrium properties of the system is now a matter solving the self-consistent set of Eqs. (16a)–(16e) while setting η_{mf} and λ equal to zero. To do this, we first need to extract the distributions $\eta_{f,m}$ from the Green functions D^{GMF} and G_F^{GMF}. To avoid taking a distracting detour here, we refer the reader to the Appendix for details. As in the previous section, we will consider a mixture composed of a free gas of fermionic ^{40}K atoms, with a density of 8.2×10^{14} cm^{-3}, and a gas of condensed ^{87}Rb bosons with density 4.9×10^{15} cm^{-3} (corresponding to the respective Thomas-Fermi densities of 10^6 atoms of either species in the center of a 100 Hz spherical trap).

Figure 10 shows the equilibrium molecular population as a function of detuning for the 492.5 G resonance. For the densities assumed, the mean-field parameter $\epsilon_{\mathrm{SM}}=g^2 n_b/E_f^2 \approx 0.4$ is indeed perturbative. For this narrow resonance, the agreement between mean-field and generalized mean-field theory is quite good, and we could as easily have used the bare molecular positions to calculate this quantity. However, the situation is completely different for the wide resonance at 544.7 G, for which the equilibrium molecular populations are shown in Fig. 11. Here the "perturbative" parameter has the value $\epsilon_{\mathrm{SM}}=38.7$, and is not perturbative at all. For a given small detuning, the simple mean-field approximation would greatly overestimate the number of molecules in the

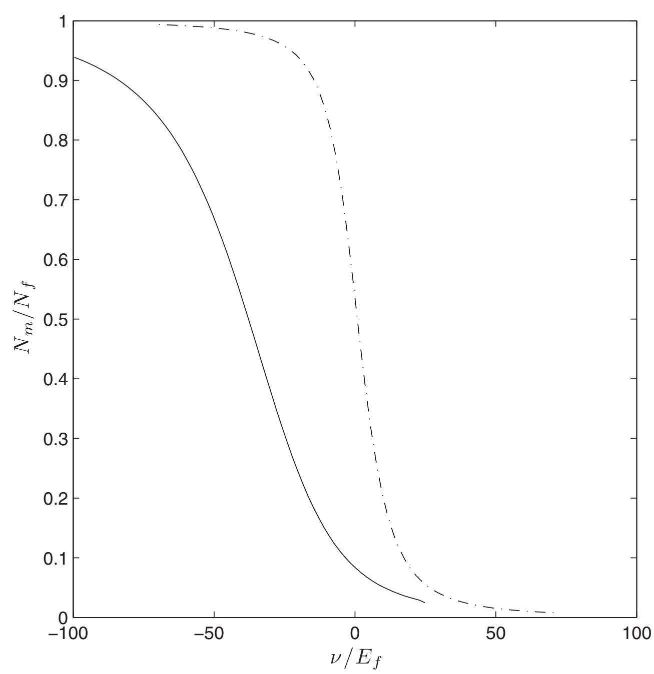

FIG. 11. Equilibrium molecular population as a function of detuning for the wider 544.7 G resonance. The solid line represents results obtained via the generalized mean-field theory presented in the text, while the dashed-dotted line represents the mean-field results.

gas at equilibrium. The more realistic generalized mean-field theory accounts for the fact that the actual molecular bound-state energy is higher than the bare detuning. This fact in turn hinders molecular formation, according to chemical potential arguments analogous to those in Sec. III B.

V. MOLECULE FORMATION

Moving beyond equilibrium properties, we are also interested in the prospects for molecule creation upon ramping a magnetic field across the resonance. In Ref. [56], the mean-field equations of motion for the system at hand were derived as follows:

$$i\hbar\frac{\partial}{\partial t}\phi=(V_{\mathrm{bg}}\rho_F+\gamma|\phi|^2)\phi+g\rho_{\mathrm{MF}}^{*}, \tag{33a}$$

$$\hbar\frac{\partial}{\partial t}\eta_F(p)=-2g\,\mathrm{Im}[\phi\eta_{\mathrm{MF}}(p)], \tag{33b}$$

$$\hbar\frac{\partial}{\partial t}\eta_M(p)=2g\,\mathrm{Im}[\phi\eta_{\mathrm{MF}}(p)], \tag{33c}$$

$$i\hbar\frac{\partial}{\partial t}\eta_{\mathrm{MF}}(p)=[\epsilon_p^F-\epsilon_p^M-\nu+V_{\mathrm{bg}}|\phi|^2]\eta_{\mathrm{MF}}(p)-g\phi^*[\eta_F(p)-\eta_M(p)], \tag{33d}$$

where $\eta_F(p)=\langle\hat{a}_p^\dagger\hat{a}_p\rangle$ is the fermionic distribution, $\eta_M(p)$ its molecular counterpart, and $\rho_{M,F}=\int\frac{dp}{2\pi^2}p^2\eta_{M,F}(p)$ the fermionic and molecular densities. Similarly, $\eta_{\mathrm{MF}}(p)=\langle\hat{c}_p^\dagger\hat{a}_p\rangle$ and is the distribution for molecule-fermion correlation, with the associated density ρ_{MF}.

Reference [56] outlined the limitations of the nonequilibrium theory by claiming that to obtain the correct two-body physics in the low-density limit, it would be necessary to include three-point and possibly higher correlations. While this fact is indeed true, we have amended it in the previous section. For experimentally reasonable parameters, the mean-field theory can be complemented by the correct renormalized propagator to accurately describe the equilibrium properties of the gas. Encouraged by this argument, we now apply it to the problem of a field ramp as well.

In the following, we wish to study molecular formation via a time-dependent ramp of the magnetic field across the resonance. To this end we use two approaches: the first consists of propagating Eqs. (33a)–(33d), ramping the detuning linearly in time from a large positive value to a large negative one, and plotting the final molecular population as a function of detuning ramping rate R. The second approach consists in noticing that if $\nu(t)$ is a linear function of time, then the mean-field Hamiltonian [Eq. (22)] is ideally suited to a Landau-Zener treatment, whereby the final molecular population as a function of detuning can be readily written as

$$n_m/\min(n_b,n_f)=1-e^{-R/\tau}. \tag{34}$$

Here $n_m/\max(n_b,n_f)$ is the fraction of possible molecules formed, and $R=1/\frac{\partial B}{\partial t}$ is the inverse ramp rate, and the exponential time constant is given by $\tau=\frac{\hbar\delta_B}{g^2n_b}=\frac{m_{\mathrm{bf}}}{ha_{\mathrm{bg}}n_b\Delta_B}$, where a_{bg} is the background scattering length, h is Planck's constant, and Δ_B is the magnetic-field width of the resonance.

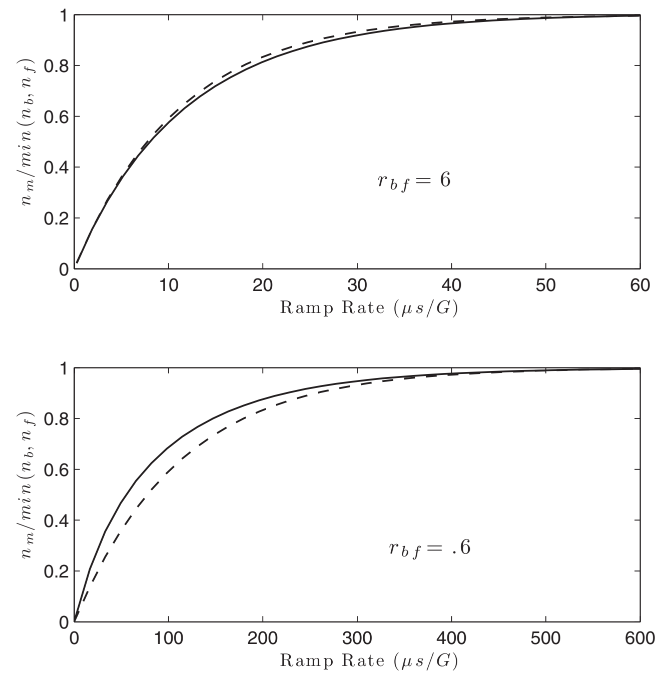

FIG. 12. Transition probability into molecular state via a magnetic-field ramp across the 492.5 G Feshbach resonance. The solid lines are obtained via numerical solutions of Eqs. (33a)–(33d), while the dashed lines represent the Landau-Zener equivalent. In the top panel, the gas is composed of more bosons than fermions, r_{bf}=6, while in the bottom panel the opposite is true, r_{bf}=0.6.

Remarkably, the characteristic sweep rate τ does not depend on the fermionic density. This arises from the fact that in mean-field theory, the momentum states of the fermionic gas are uncoupled, except via the depletion of the condensate. Since in the Landau-Zener approach the depletion is assumed small, it follows that the various fermionic momentum states are considered independently, and thus the probability of transition of the gas is equal to the probability of transition of each individual momentum state. This approximation is only valid for narrow resonances, such as the 492.5 G resonance in Table I.

Molecular formation rate versus ramp rate is shown in Fig. 12 for the cases r_{bf}=6 (more fermions than bosons) and r_{bf}=0.6 (more fermions than bosons). In both cases, the Landau-Zener result agrees nearly perfectly with direct numerical integration. This agreement is surprising in the case of more fermions, since the width of the crossing is proportional to the density of leftover bosons, and we expect that this number will change substantially as the bosonic population is depleted via the formation of molecules. This type of time-dependent crossing should not be properly described by the Landau-Zener formula. However, monitoring the time evolution of the molecular population as a function of time shows that the majority of the transfer takes place quite abruptly somewhat after crossing the zero-detuning region, whereby the change in bosonic density does not modify the energy levels substantially.

VI. CONCLUSION

In this paper, we developed and solved a generalized mean-field theory describing an ultracold atomic Bose-Fermi mixture in the presence of an interspecies Feshbach resonance. The theory is "generalized" in the sense that it correctly incorporates bosonic fluctuations, at least to the level that it reproduces the correct two-body physics in the extreme dilute limit. This theory, like any mean-field theory, presents undeniable limitations. Nevertheless, any useful many-body treatment must start from a well conceived mean-field theory. Future directions of this work should include the generalization to finite temperature and the inclusion of a trap, initially in a local-density approximation. These advances would be essential to check for empirical confirmation of the theory.

ACKNOWLEDGMENT

D.C.E.B. and J.L.B. acknowledge support from the DOE and the Keck Foundation.

APPENDIX: GREEN-FUNCTION METHODS FOR FERMIONS

In this appendix, we briefly introduce some of the Green-function techniques that we found useful in our calculations.

1. Free Green functions

We start from the Green function for a gas of free fermions, which is given, in the frequency-momentum representation, by

$$G^0(w,\mathbf{q}) = \frac{1}{\omega - \xi(\mathbf{p}) + i\eta\,\mathrm{sgn}[\xi(\mathbf{p})]}, \tag{A1}$$

where $\xi(\mathbf{p}) = \mathbf{p}^2/2m - \mu$. The momentum distribution, at equilibrium, is given by

$$n(\mathbf{p}) = -i \lim_{\eta\to 0^+} \int \frac{d\omega}{2\pi} e^{i\omega\eta} G^0(w,\mathbf{q}). \tag{A2}$$

Here the limit comes from the equilibrium condition; the frequency, in the Green-function definition, is the Fourier space equivalent of time, whereby the real-time Green function represents the evolution of the system from time t to t', and the observables obtained this way represent expected values of the kind $\langle \psi(t)|O|\psi(t')\rangle$. However, since we want equilibrium conditions, we need to take the limit $t\to t'$, which is nontrivial, since G^0 is defined by a Green-function equation of the form $\mathcal{L}G^0(t-t') \propto \delta(t-t')$, where $\mathcal{L}$ is some linear operator, and which highlights a peculiar behavior in the limit we desire. However, since we know on physical grounds that observables such as the momentum distribution must be defined and well behaved at equilibrium, then by first taking the expectation value integral, and then the limit, we can circumvent the problem. In Eq. (A2), this implies that we cannot quite get rid of the Fourier transform exponent $e^{i\omega(t-t')}$ until after the ω integral.

To perform the integral in Eq. (A2), we exploit the Fourier exponent by noting that since η is positive, $e^{i\omega\eta}\to 0$ as $\omega\to +i\infty$, so that the integral is identical to a contour integral over the path defined by the real ω axis, closed in the upper complex ω plain by an infinite radius semicircle, which, as we have just seen, gives no contribution to the integral. We can now integrate using the residue theorem.

We note that the integrand in Eq. (A2) has a simple pole at $\omega = \xi(\mathbf{p}) - i\eta\,\mathrm{sgn}[\xi(\mathbf{p})]$. Thus, if $\xi(\mathbf{p}) > 0$, then the pole is in the lower complex plane, and the integral vanishes, and if $\xi(\mathbf{p}) > 0$, then the pole is in the upper complex plane, with residue 1. Using the residue theorem, and summarizing these results, we finally get

$$n(\mathbf{p}) = \Theta(-\xi(\mathbf{p})), \tag{A3}$$

which we recognize as the zero-temperature Fermi distribution.

2. Interacting Green functions

According to Dyson's equation, the Green function for an interacting system has the form

$$G(w,\mathbf{q}) = \frac{1}{\omega - \xi(\mathbf{p}) - \Sigma(\omega,\mathbf{p})}, \tag{A4}$$

where $\Sigma(\omega,\mathbf{p})$ is an arbitrarily complicated function summarizing all the interactions in the system, which is known as self-energy.

The prescription to find Σ is quite straightforward, and it consists of adding all amputated connected Feynman diagrams for the system. The fact that, in general, the number of such diagrams is infinite makes this task virtually impossible. Nonetheless, Eq. (A4) is very powerful since it allows one to include the effect of infinite subsets of the total number of diagrams in the system by only having to explicitly calculate a few representative ones.

An alternative standard approach leads to the exact result (note: Abrikosov measures energy from μ; here we measure from 0, which is more standard)

$$G(\omega,\mathbf{p}) = \int_0^\infty d\omega' \left[\frac{A(\omega,\mathbf{p})}{\omega - \omega' + i\eta} + \frac{B(\omega,\mathbf{p})}{\omega + \omega' - i\eta}\right], \tag{A5}$$

where A and B are, again, arbitrary complicated functions, though they are known to be finite.

To understand A and B more closely, we need to introduce the following well-known identity:

$$\lim_{\nu\to 0} \frac{1}{x \pm i\nu} = \mathrm{P}\frac{1}{x} \mp i\pi\delta(x), \tag{A6}$$

where P is a Cauchy principal value, which represents the contribution due to a discontinuity in a Riemann sheet (branch cut), and the δ function represents the contribution due to the pole.

Applying Eq. (A6) to Eq. (A5), we get

$$\mathrm{Re}\, G(\omega,\mathbf{p}) = \mathrm{P}\int_0^\infty d\omega' \left[\frac{A(\omega,\mathbf{p})}{\omega - \omega' + i\eta} + \frac{B(\omega,\mathbf{p})}{\omega + \omega' - i\eta}\right], \tag{A7}$$

$$\mathrm{Im}\, G(\omega,\mathbf{p}) = \begin{cases} -\pi A(\omega,\mathbf{p}) & \text{if } \omega > 0 \\ \pi B(-\omega,\mathbf{p}) & \text{if } \omega < 0. \end{cases} \tag{A8}$$

Finally, Eq. (A2) represents a fundamental property of Green functions, and it can be generalized to interacting systems simply substituting G^0 with G. Applying it to Eq. (A5), and performing the ω integral first, we get

$$n(\mathbf{p}) = \int_0^\infty d\omega' B(\omega,\mathbf{p}) = \int_{-\infty}^0 d\omega \frac{-1}{\pi}\, \mathrm{Im}\, G(\omega,\mathbf{p}). \tag{A9}$$

Introducing the function $\rho(\omega,\mathbf{p}) = -2\, \mathrm{Im}\, G(\omega,\mathbf{p})$, generally called the spectral function, the above equation can be written as

$$n(\mathbf{p}) = \int \frac{d\omega}{2\pi}\rho(\omega,\mathbf{p})\Theta(-\omega). \tag{A10}$$

An important property of the spectral function is that for all $\mathbf{p}$,

$$\int \frac{d\omega}{2\pi}\rho(\omega,\mathbf{p}) = 1. \tag{A11}$$

This can be understood as a sum rule in the following sense: if we wish to calculate the number of holes in the system, we would take the $\eta \to 0^-$ limit in Eq. (A2). The distribution would then have been $n_{\mathrm{holes}}(\mathbf{p}) = 1 - n(\mathbf{p}) = \int_0^\infty d\omega' A(\omega',\mathbf{p})$, so that $1 = \int_0^\infty d\omega'[A(\omega',\mathbf{p}) + B(\omega',\mathbf{p})] = \int \frac{d\omega}{2\pi}\rho(\omega,\mathbf{p})$.

Using Eq. (A4), together with the definition of ρ, we can write

$$\rho(\omega,\mathbf{p}) = \frac{-2\, \mathrm{Im}\, \Sigma(\omega,\mathbf{p})}{[\omega - \xi(\mathbf{p}) - \mathrm{Re}\, \Sigma(\omega,\mathbf{p})]^2 + [\mathrm{Im}\, \Sigma(\omega,\mathbf{p})]^2}. \tag{A12}$$

Furthermore, if Σ were to be real, or if, equivalently, the pole of the Green function were to be real, for some momentum $\mathbf{p}$, then taking the limit $\mathrm{Im}\, \Sigma \to 0$ of Eq. (A4), and using Eq. (A6), we get

$$\rho(\omega,\mathbf{p}) = 2\pi\delta(\omega - \xi(\mathbf{p}) - \mathrm{Re}\, \Sigma(\omega,\mathbf{p})), \tag{A13}$$

which can be simplified, using the properties of the δ function, to

$$\rho(\omega,\mathbf{p}) = 2\pi Z(\mathbf{p})\delta(\omega - \omega_0(\mathbf{p})), \tag{A14}$$

where Z, known as spectral weight, is given by

$$Z(\mathbf{p}) = \frac{1}{\left| 1 - \frac{\partial}{\partial\omega}\mathrm{Re}\, \Sigma(\omega,\mathbf{p}) \right|_{w=\omega_0(\mathbf{p})}}, \tag{A15}$$

and $\omega_0(\mathbf{p})$ is the pole of the Green function, defined by

$$\omega_0(\mathbf{p}) - \xi(\mathbf{p}) - \Sigma(\omega_0(\mathbf{p}),\mathbf{p}) = 0. \tag{A16}$$

The momentum distribution in this case is thus given by

$$n(\mathbf{p}) = Z(\mathbf{p}) \int \delta(\omega - \omega_0(\mathbf{p}))\Theta(-\omega) = Z(\mathbf{p})\Theta(-\omega_0(\mathbf{p})). \tag{A17}$$

[1] J. Bardeen, L. N. Cooper, and J. R. Schrieffer, Phys. Rev. **108**, 1175 (1957).
[2] S. N. Bose, Z. Phys. **26**, 178 (1924).
[3] A. Einstein, Sitzungsber. Preuss. Akad. Wiss., Phys. Math. Kl. **22**, 261 (1924).
[4] M. Greiner, C. A. Regal, and D. S. Jin, Nature **426**, 537 (2003).
[5] M. Bartenstein, A. Altmeyer, S. Riedl, S. Jochim, C. Chin, J. H. Denschlag, and R. Grimm, Phys. Rev. Lett. **92**, 120401 (2004).
[6] M. W. Zwierlein, C. A. Stan, C. H. Schunck, S. M. F. Raupach, A. J. Kerman, and W. Ketterle, Phys. Rev. Lett. **92**, 120403 (2004).
[7] E. A. Donley, N. R. Claussen, S. T. Thompson, and C. E. Wieman, e-print arXiv:cond-mat/0204436.
[8] S. Inouye, J. Goldwin, M. L. Olsen, C. Ticknor, J. L. Bohn, and D. S. Jin, Phys. Rev. Lett. **93**, 183201 (2004).
[9] F. Ferlaino, C. D'Errico, G. Roati, M. Zaccanti, M. Inguscio, G. Modugno, and A. Simoni, Phys. Rev. A **73**, 040702(R) (2006).
[10] C. A. Stan, M. W. Zwierlein, C. H. Schunck, S. M. F. Raupach, and W. Ketterle, Phys. Rev. Lett. **93**, 143001 (2004).
[11] J. J. Zirbel, K.-K. Ni, S. Ospelkaus, J. P. D'Incao, C. E. Wieman, J. Ye, and D. S. Jin, Phys. Rev. Lett. **100**, 143201 (2008).
[12] Yong-il Shin, A. Schirotzek, C. H. Schunck, and W. Ketterle, Phys. Rev. Lett. **101**, 070404 (2008).
[13] C. Ospelkaus, S. Ospelkaus, L. Humbert, P. Ernst, K. Sengstock, and K. Bongs, Phys. Rev. Lett. **97**, 120402 (2006).
[14] R. Roth and H. Feldmeier, Phys. Rev. A **65**, 021603(R) (2002).
[15] R. Roth, Phys. Rev. A **66**, 013614 (2002).
[16] G. Modugno, G. Roati, F. Riboli, F. Ferlaino, R. J. Brecha, and M. Inguscio, Science **297**, 2240 (2002).
[17] H. Hu and X.-J. Liu, Phys. Rev. A **68**, 023608 (2003).
[18] X.-J. Liu, M. Modugno, and H. Hu, Phys. Rev. A **68**, 053605 (2003).
[19] L. Salasnich, S. K. Adhikari, and F. Toigo, Phys. Rev. A **75**, 023616 (2007).
[20] P. Pedri and L. Santos, Phys. Rev. Lett. **95**, 200404 (2005).
[21] Sadhan K. Adhikari, Phys. Rev. A **70**, 043617 (2004).
[22] H. P. Büchler and G. Blatter, Phys. Rev. A **69**, 063603 (2004).
[23] R. Kanamoto and M. Tsubota, Phys. Rev. Lett. **96**, 200405 (2006).
[24] S. K. Adhikari, Phys. Rev. A **72**, 053608 (2005).
[25] A. Albus, F. Illuminati, and J. Eisert, Phys. Rev. A **68**, 023606 (2003).
[26] M. Lewenstein, L. Santos, M. A. Baranov, and H. Fehrmann, Phys. Rev. Lett. **92**, 050401 (2004).
[27] R. Roth and K. Burnett, Phys. Rev. A **69**, 021601(R) (2004).
[28] A. Sanpera, A. Kantian, L. Sanchez-Palencia, J. Zakrzewski,

and M. Lewenstein, Phys. Rev. Lett. **93**, 040401 (2004).
[29] K. Günter, T. Stöferle, H. Moritz, M. Köhl, and T. Esslinger, Phys. Rev. Lett. **96**, 180402 (2006).
[30] I. Titvinidze, M. Snoek, and W. Hofstetter, Phys. Rev. Lett. **100**, 100401 (2008).
[31] M. J. Bijlsma, B. A. Heringa, and H. T. C. Stoof, Phys. Rev. A **61**, 053601 (2000).
[32] H. Heiselberg, C. J. Pethick, H. Smith, and L. Viverit, Phys. Rev. Lett. **85**, 2418 (2000).
[33] D. V. Efremov and L. Viverit, Phys. Rev. B **65**, 134519 (2002).
[34] L. Viverit, Phys. Rev. A **66**, 023605 (2002).
[35] F. Matera, Phys. Rev. A **68**, 043624 (2003).
[36] A. P. Albus, S. A. Gardiner, F. Illuminati, and M. Wilkens, Phys. Rev. A **65**, 053607 (2002).
[37] D.-W. Wang, Phys. Rev. Lett. **96**, 140404 (2006).
[38] S. Powell, S. Sachdev, and H. P. Büchler, Phys. Rev. B **72**, 024534 (2005).
[39] A. Storozhenko, P. Schuck, T. Suzuki, H. Yabu, and J. Dukelsky, Phys. Rev. A **71**, 063617 (2005).
[40] Eddy Timmermans, Paolo Tommasini, Mahir Hussein, and Arthur Kerman, Phys. Rep. **315**, 199 (1999).
[41] S. J. J. M. F. Kokkelmans and M. J. Holland, Phys. Rev. Lett. **89**, 180401 (2002).
[42] S. J. J. M. F. Kokkelmans, J. N. Milstein, M. L. Chiofalo, R. Walser, and M. J. Holland, Phys. Rev. A **65**, 053617 (2002).
[43] Y. Ohashi and A. Griffin, Phys. Rev. Lett. **89**, 130402 (2002).
[44] R. A. Duine and H. T. C. Stoof, J. Opt. B: Quantum Semiclassical Opt. **5**, S212 (2003).
[45] E. M. Lifshitz and L. P. Pitaevskii, *Statistical Physics*, Part 2 (Butterworth-Heinemann, Oxford, UK, 1996).
[46] C. Zener, Proc. R. Soc. London, Ser. A **137**, 696 (1932).
[47] L. D. Landau, Phys. Z. Sowjetunion **1**, 89 (1932).
[48] R. A. Duine and H. T. C. Stoof, Phys. Rep. **396**, 115 (2004).
[49] Thorsten Köhler, Thomas Gasenzer, and Keith Burnett, Phys. Rev. A **67**, 013601 (2003).
[50] M. Holland, S. J. J. M. F. Kokkelmans, M. L. Chiofalo, and R. Walser, Phys. Rev. Lett. **87**, 120406 (2001).
[51] G. M. Falco and H. T. C. Stoof, Phys. Rev. Lett. **92**, 130401 (2004).
[52] A. V. Andreev, V. Gurarie, and L. Radzihovsky, Phys. Rev. Lett. **93**, 130402 (2004).
[53] Y. Ohashi and A. Griffin, Phys. Rev. A **67**, 033603 (2003).
[54] A. V. Avdeenkov, J. Phys. B **37**, 237 (2004).
[55] A. V. Avdeenkov and J. L. Bohn, Phys. Rev. A **71**, 023609 (2005).
[56] D. C. E. Bortolotti, A. V. Avdeenkov, C. Ticknor, and J. L. Bohn, J. Phys. B **39**, 189 (2006).
[57] A. V. Avdeenkov, D. C. E. Bortolotti, and J. L. Bohn, Phys. Rev. A **74**, 012709 (2006).
[58] R. G. Newton, *Scattering Theory of Waves and Particles*, 2nd ed. (Springer–Verlag, Berlin, 1982).
[59] J. W. Negele and H. Orland, *Quantum Many-Particle Systems* (Addison-Wesley, Reading, MA, 1988).
[60] D. C. E. Bortolotti (unpublished).
[61] B. Marcelis, E. G. M. van Kempen, B. J. Verhaar, and S. J. J. M. F. Kokkelmans, Phys. Rev. A **70**, 012701 (2004).